PERGAMON

Scripta mater. 42 (2000) 597–602

Scripta MATERIALIA

www.elsevier.com/locate/scriptamat

A NEW CLASS OF ULTRA-HARD MATERIALS BASED ON $AlMgB_{14}$

B. A. Cook, J. L. Harringa, T. L. Lewis, and A. M. Russell
Ames Laboratory, Iowa State University, Ames, IA, 50011, USA

(Received November 8, 1999)
(Accepted November 12, 1999)

Keywords: Hard materials; Mechanical alloying; Complex borides

Introduction

It has long been known that the hardest materials possess strongly bonded crystal structures of high symmetry. Hardness is a function of both the strength of the interatomic bonding and of the rigidity of the lattice framework. Diamond is the hardest known bulk material (approximately 70 GPa), due to strong covalent sp^3 bonding in a tetrahedral lattice configuration. The cF8 structure of diamond is also found in many of the other ultra-hard materials such as cubic-BN and several of the tetravalent metal carbides.

In this study, aluminum magnesium boride combined with 5 to 30 mol.% additives ($AlMgB_{14}$:X where X = Si, P, C, AlN, TiB_2, or BN), were prepared by mechanical alloying and consolidated by vacuum hot pressing. Matkovich and Economy (1) first reported the orthorhombic $AlMgB_{14}$ intermetallic compound (oI64, space group Imam, a = 0.5848 nm, b = 0.8112 nm, c = 1.0312 nm), and the structure determination was later refined by Higashi and Ito (2). The unit cell is based on four B_{12} icosahedral units centered at (0, 0, 0), (0, 0.5, 0.5), (0.5, 0, 0), and (0.5, 0.5, 0.5) within the unit cell. The remaining eight B atoms lie outside the icosahedra, bonding to the icosahedral B atoms and to the Al and Mg atoms. The Al atoms occupy a four-fold position at (0.250, 0.750, 0.250), and the Mg atoms occupy a four-fold position at (0.250, 0.359, 0). The icosahedra are arranged in distorted, close-packed layers. The unique electronic, optical, and mechanical properties of this material are due to a complex interaction within each icosahedron (intrahedral bonding) combined with interaction between the icosahedra (intericosahedral bonding).

Prior work on this complex orthorhombic boride has mainly involved determination of crystal structure. Bairamashvili and co-workers (3) initially examined the thermoelectric properties of this and related borides prepared by hot pressing powders produced from crystallization of aluminum melt solutions. They observed that these compounds exhibited high melting points and were relatively brittle. More recently, Werheit, *et al.* (4) examined the optical and electronic properties of the orthorhombic $AlMgB_{14}$ prepared by growing single crystals in alumina crucibles from Al-B solutions containing Li or Mg. In addition to their unique mechanical properties, evidence suggests that these systems exhibit novel electronic properties such as hopping conduction (5). Crystallographic studies indicate that the metal sites are not fully occupied in the lattice so that the true chemical formula may be closer to $Al_{0.75}Mg_{0.78}B_{14}$. Table 1 provides a comparison with several hard materials along with their corresponding density, bulk, and shear moduli (6).

PII: S1359-6462(99)00400-5

TABLE 1
Density, Hardness, Bulk and Shear Moduli of Selected Hard Materials

	Density (g/cm^3)	Hardness (GPa)	Bulk Modulus (GPa)	Shear Modulus (GPa)
C (diamond)	3.52	70	443	535
BN (cubic)	3.48	45–50	400	409
C_3N_4 (cubic)	†	40–55	496	332
SiC	3.22	24–28	226	196
Al_2O_3	3.98	21–22	246	162
TiB_2	4.50	30–33	244	263
WC	15.72	23–30	421	
TiC	4.93	28–29	241	188
AlB_{12}	2.58	26		
Si_3N_4	3.19	17–21	249	123
$AlMgB_{14}$	2.66	32–35*		
$AlMgB_{14}$ + Si	2.67	35–40*		
$AlMgB_{14}$ + TiB_2	2.70	40–46*		

* Hardness values from this study.
†Presently available in quantities too small to permit measurement of bulk density.

Experimental Procedure

This study was performed to determine conditions for preparation and consolidation of the $AlMgB_{14}$-based materials from elemental constituents using mechanical alloying. Results indicated that the microstructure and hardness of these materials were strongly dependent on processing conditions. Mechanical alloying was used to produce fine powder, suitable for pressure-assisted sintering to nearly full density. However, different milling conditions resulted in a variation in the volume fraction of microporosity in hot pressed compacts due to differences in particle morphology.

Microhardness was measured with a Wilson-Tukon model 200 equipped with state-of-the-art CCD image enhancement capability. Standard samples of near-zero porosity SiC and cubic-BN were measured with this hardness testing unit and found to match published hardness values.

A significant portion of this project was devoted to development and optimization of a suitable method for preparing $AlMgB_{14}$ with no other elements added (hereinafter referred to as "baseline" material) and consolidation of the powder into a dense compact. Mechanical alloying (MA) was employed because of its ability to generate fine, sinterable powders. As the particle size is reduced, diffusion distances become smaller, thereby enhancing sintering. An additional benefit of mechanical alloying is the high surface-to-volume ratio which promotes chemical reactivity and compound formation. Prior research with this technique has demonstrated that reasonably good control of oxygen impurities can be obtained by restricting handling of the powders to an inert glove box environment with less than 1 ppm O. In fact, less than 0.5 at. % increase in O, as determined by neutron activation, was observed during an entire MA-to-hot pressing sequence when steel vials with o-ring seals were employed in the preparation of Si-Ge materials (7).

The large number of independent variables complicates identification of an optimum processing route. These variables include milling type (vibratory vs. planetary vs. attritor), vial geometry (convex curvature vs. flat-ended), ball-to-charge weight ratio, milling atmosphere, milling time, and type of precursor material (powders vs. chunks). Thirty combinations of these parameters were examined in an attempt to approach the optimum processing method. Consolidation of the loose powder was accomplished by hot pressing in BN-lined graphite dies. Various temperatures within the range of 1573 to 1773 K were evaluated in order to determine the optimum for consolidation. After cooling and removal

of the die from the hot press, the consolidated samples were ejected, and the BN protective coating was abraded off. A total of twenty-seven hot pressings were performed. Apparent density of the bulk compacts was determined using an Archimedes immersion technique, and most of the samples pressed at 1673 K had a density of 98% of theoretical density (2.6 g/cm^3).

In addition to the stoichiometric materials discussed above, several $AlMgB_{14}$-based compounds were prepared with additions of elemental Si, P, or C and with the compounds TiB_2, AlN, and BN. Samples were prepared in the same manner as the stoichiometric "baseline" materials except that 5 to 30 mol.% of the additive was added to the initial powder charge.

One of the key industrial concerns for an abrasive material is its chemical activity with the workpiece. Chemical reactivity with Fe and Ti was studied by preparing diffusion couples, subjecting them to various combinations of high temperature and high pressure, and subsequently examining them by SEM. Two configurations were studied; one in which a piece of fully dense $AlMgB_{14}$ was sandwiched between 1 mm thick iron and Ti disks, the other in which the boride was positioned directly below a 6.35 mm dia. steel rod segment. The boride surfaces were prepared by grinding against a series of progressively finer diamond polishing wheels and rinsed with hexane between steps. The Fe and Ti surfaces were also polished and rinsed with hexane prior to assembly of the sandwich. The components were positioned inside a graphite die which was in turn positioned in a high temperature graphite furnace. The tests were all conducted under vacuum conditions (10^{-6} T) and a light load was applied to the die ($\sim$1–2 MPa) in order to hold the components in intimate contact. The temperature of the furnace was ramped at 0.17 K/s to a soak point of 1273 to 1573 K and held for 7200 s. One of the diffusion couples, prepared at a temperature of 1473 K for 7200 s, was sectioned with a high speed diamond saw, mounted in diallylphthalate resin along with Al and Mg standards, and polished to 0.25 μm.

Results

The best quality baseline material produced in this study exhibited microhardness in the range of 32 to 35 GPa. These values are significantly higher than the hardness reported by other investigators who grew $AlMgB_{14}$ single crystals from high temperature solutions (e.g. Higashi, et alia (8) reported a hardness value of 27.4 to 28.3 GPa for $AlMgB_{14}$). Typical grain size for the hot pressed alloys was 5 to 20 microns. Therefore, it is unlikely that the increase in hardness is directly related to the microstructure, as in the case of nanophase materials. Addition of Si and TiB_2 resulted in the microhardness values listed in Table 1. The highest hardness was observed in a sample prepared with 30 wt. % TiB_2, which gave hardness values of 46 GPa, comparable to cubic boron nitride, and clearly placing these materials in the "ultra-hard" category. Additional samples containing P, C (in the form of fullerite), AlN, and h-BN have been synthesized but not yet characterized for microhardness.

An X-ray study of the powder at various stages of processing was conducted in order to determine whether alloy formation occurs during MA, or whether MA simply reduces particle size (and hence diffusion distances) which in turn facilitates compound formation during hot pressing. The x-ray patterns were obtained on a small quantity of powder removed from the vials in an He-filled glove bag at regular intervals. Considerable line broadening was observed during MA, indicating the presence of strain (cold work) in the Al and Mg and particle size refinement. Analysis of the pattern after 20 hours of processing indicated that the material is nanocrystalline, with the presence of a few low intensity peaks corresponding to the individual components. X-ray patterns indicate that no significant amount of $AlMgB_{14}$ forms during milling, although a small amount of FeB_{49} was observed, presumably due to interaction with wear debris from the high energy milling process. The x-ray pattern of samples containing TiB_2 were found to have reflections indexed to both the orthorhombic-$AlMgB_{14}$ and hexagonal-TiB_2 phases.

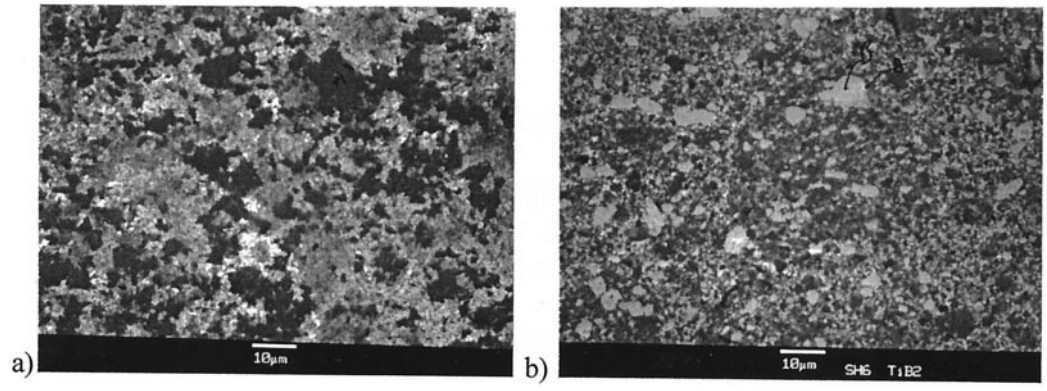

Figure 1. a) Back-scattered electron SEM image of $AlMgB_{14}$ prepared by mechanical alloying and hot pressed. b) BSE micrograph of $AlMgB_{14}$ with 30% TiB_2. The bright spots are regions high in TiB_2 concentration. The dark regions correspond to $AlMgB_{14}$.

An SEM backscattered electron image of a typical baseline sample consolidated by hot pressing is shown in Figure 1a. At this magnification, it is clear that the microstructure is highly heterogeneous, with regions of widely varying phase contrast. An EDS spectrum was obtained from both the light and dark regions; the dark areas were found to correspond to $AlMgB_{14}$ while the lighter contrast regions contain $AlMgB_{14}$ and Fe. A higher magnification BSE image of one of the lighter regions is shown in Figure 2a. The bright areas, identified as points "B" and "C" in the photo, contain high concentrations of Fe, in addition to the baseline material. The composition at point "A" appears closer to that of the nominal alloy. What is remarkable about the microstructure is the fine distribution of phases at a sub-micron level. A high magnification image shows that compositional contrast exists down to a scale of 100 nm. This material clearly contains large-scale inclusions, on the order of 10 microns, however, the largest volume fraction is composed of a nanoscale composite.

An SEM backscattered electron image of a boride-Fe diffusion couple interface is shown in Figure 3a. The bright region on the right side corresponds to the Fe while the darker region on the left corresponds to the boride. A large number of bright spots are observed on the boride side and EDS analysis indicates that these spots are predominantly Fe, presumably wear debris from the mechanical

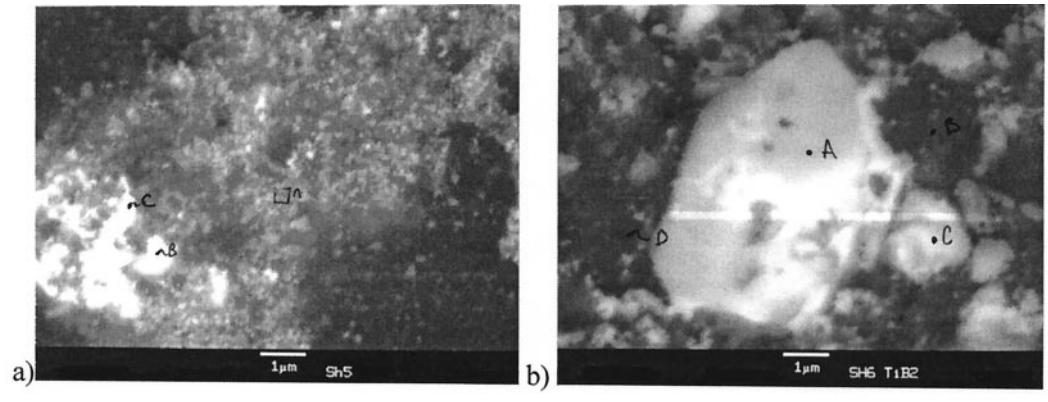

Figure 2. a) High-magnification BSE SEM image of baseline $AlMgB_{14}$ material. b) BSE image of $AlMgB_{14}$ with 30% TiB_2 added. The bright spot labeled "A" in the micrograph corresponds to a region high in TiB_2 concentration. The dark regions correspond to $AlMgB_{14}$. The interface between TiB_2 and matrix appears to be a reaction zone enriched in Ti and Si.

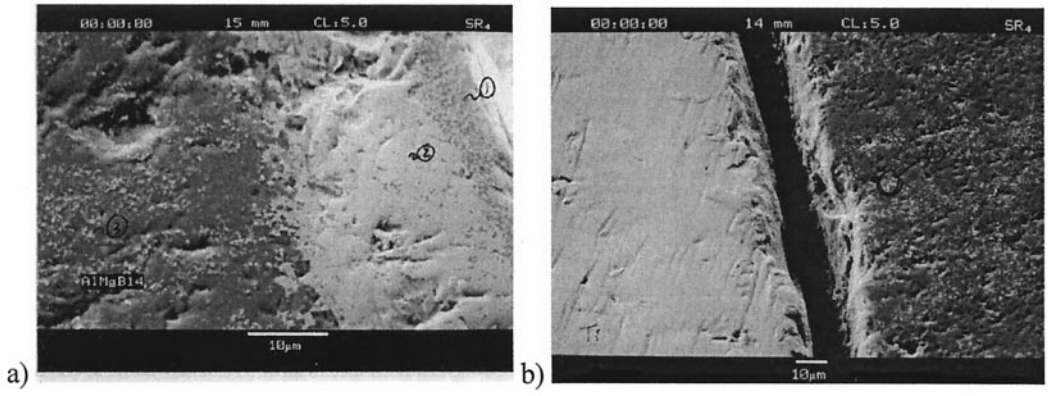

Figure 3. a) Back-scattered electron SEM image of Fe-$AlMgB_{14}$ interface after a 7200 s heat treatment at 1473 K. The bright region on the right is Fe. b) Back-scattered electron SEM image of Ti-$AlMgB_{14}$ interface after a 7200 s heat treatment at 1473 K. The bright region on the left is Ti.

alloying process. These spots extend throughout the entire boride specimen. The presence of the irregular interface suggests that some diffusion between the components occurred. In contrast, Figure 3b shows the corresponding boride-Ti interface in which complete debonding occurred during cooling with formation of a 10 μm gap between the materials. No locations exhibited indication of reaction between the boride and Ti.

A dramatic improvement in hardness was found to result from addition of TiB_2. Baseline samples as discussed above were weighed out and milled along with 20 to 30 wt. percent TiB_2. The microhardness of these compacts was found to range from 38 GPa to 46 GPa. The material was examined in a scanning electron microscope and considerable microstructural refinement was observed, as shown in Figure 1b, compared with the baseline alloy. A high density of second phase is distributed uniformly throughout the material, as shown in the backscattered image. SEM/EDS analysis of these inclusions shows that they consist primarily of TiB_2, although a reaction zone appears to have formed between this phase and the matrix, enriched in Ti and Si. The microhardness values for these specimens were considerably higher than previously measured, with the upper bound approximately equal to or slightly higher than that of cubic boron nitride. A higher magnification image of one of the TiB_2-rich regions is shown in Figure 2b. The darker matrix phase was found to consist of $AlMgB_{14}$ and TiB_2 while the bright region appears to be exclusively TiB_2. The lighter micron-sized phases contain both baseline and TiB_2, albeit in varying ratios.

Discussion

These $AlMgB_{14}$-based materials are unexpectedly hard. The conventional paradigm for ultra-hard materials calls for a simple, symmetric, isotropic crystal structure. Moreover, that crystal structure should possess few degrees of freedom within the unit cell to frustrate the material's ability to react to compressive loading by relaxing into another configuration that lowers total system energy. The oI64 structure of baseline $AlMgB_{14}$ is quite complex; its low symmetry, large number of atoms per unit cell, and, in some specimens, incompletely occupied atom sites all appear to contradict the accepted precepts for extreme hardness. Nevertheless, the baseline material is among the hardest substances known. An additional paradox is introduced by the observation that some additives actually increase the hardness of the material. In many hard materials, adding additional elements or compounds typically *lowers* hardness.

The reason for the increased hardness accompanying Si addition is uncertain. It may be that the Si atoms substitute for Al in the orthorhombic unit cell or occupy some of the vacant Al or Mg sites present in the Al and Mg deficient substiochiometric unit cell. It is conceivable that the slightly smaller Si atoms might give rise to a higher occupancy than the 74.8% reported by Higashi and Ito. If so, the overall intericosahedral bonding might be stronger, leading to a more rigid unit cell. Moreover, the additional electron provided by the Si would be expected to form an additional bond with the boron icosahedra. Microstructural refinement may also play a contributing factor in improving the mechanical hardness of these alloys. Structure determinations on the $AlMgB_{14}$ + Si and on the $AlMgB_{14}$ + TiB_2, along with theoretical calculations of relevant bonding energies will be needed to resolve these questions.

Theoretical predictions by Liu and Cohen (9) that the bulk modulus of the metastable, hexagonal $\beta-C_3N_4$ may exceed that of diamond, has motivated extensive experimental efforts to synthesize various carbon nitride compounds (for example, (10)). Recent evidence suggests that the cubic polymorph has a modulus exceeding that of diamond (11). However, there exists some controversy as to whether bulk modulus or shear modulus is a better indicator of a material's hardness (12). Nevertheless, all of the materials predicted to have high hardness share a common characteristic in that they involve relatively simple structures, most with high symmetry, and atoms with short, highly covalent bonds, as illustrated by the recent synthesis of cubic Si_3N_4 (13). The chemically-modified $AlMgB_{14}$ does not fit this paradigm, which raises some interesting fundamental scientific questions about the role of structural complexity in determining hardness. Additional studies of these materials by atomic force microscopy and by ultrasonic methods will be discussed in a future publication. The results of ultrasonic testing are expected to provide an indication of the bulk and shear modulus.

The highest hardness was observed in the $AlMgB_{14}$ + 30%TiB_2 material, which possesses a multi-phase microstructure. Here again, an increase in hardness accompanying the introduction of additional phases is somewhat surprising and difficult to explain. The possible compounds that may form at the $AlMgB_{14}-TiB_2$ interface during hot pressing are numerous.

Acknowledgments

The authors wish to acknowledge F. Laabs, H. Sailsbury, and M. Strange, all of Ames Laboratory, for their valuable assistance and for examining the materials used in this study. This work was performed at Ames Laboratory, operated for the U. S. Department of Energy by Iowa State University under contract no. W-7405-ENG-82. Funding was provided by the Iowa State University Center for Advanced Technology Development and also by the ISU Carver Charitable Trust.

References

1. V. I. Matkovich and J. Economy, J. Acta Crystallogr. B26, 616 (1970).
2. W. Higashi and T. Ito, J. Less Common Met. 92, 239 (1983).
3. I. A. Bairamashvili, L. I. Kekelidze, O. A. Golikova, and V. M. Orlov, J. Less Common Met. 67, 461 (1979).
4. H. Werheit, U. Kuhlmann, G. Krach, I. Higashi, T. Lundström, and Y. Yu, J. Alloys Compounds 202, 269 (1993).
5. D. Emin, Phys. Today. 1, 55 (1987).
6. D. M. Teter, MRS Bull. 23, 22 (1998).
7. B. A. Cook, J. L. Harringa, S. H. Han, and B. J. Beaudry, J. Appl. Phys. 72, 1423 (1992).
8. I. Higashi, M. Kobayashi, S. Okada, K. Hamano, and T. Lundström, J. Cryst. Growth. 128, 1113 (1993).
9. A. Y. Liu and M. L. Cohen, Science. 245, 841 (1989).
10. Z. J. Zhang, S. Fan, C. M. Lieber, Appl. Phys. Lett. 66, 3582 (1995).
11. D. M. Teter and R. J. Hemley, Science. 271, 53 (1996).
12. D. M. Teter, MRS Bull. 23, 22 (1998).
13. MRS Bull. 24, 9 (1999).